Bone Reports 12 (2020) 100271

Contents lists available at ScienceDirect

Bone Reports

journal homepage: www.elsevier.com/locate/bonr

A degenerative medial meniscus retains some protective effect against osteoarthritis-induced subchondral bone changes

G. Mitton[a], K. Engelke[c,d], S. Uk[a], J.D. Laredo[a,b], C. Chappard[a,*]

[a] B3OA, UMR CNRS 7052, Inserm U1271 Université de Paris, Paris, France
[b] Service de Radiologie, Hôpital Lariboisière, Paris, France
[c] Institute of Medical Physics, University of Erlangen-Nürnberg, Erlangen, Germany
[d] Department of Internal Medicine 3, University of Erlangen-Nuremberg and Universitätsklinikum Erlangen, Erlangen, Germany

ARTICLE INFO

Keywords:
Osteoarthritis
Meniscus
Micro-computed tomography
Cartilage
Subchondral trabecular bone

ABSTRACT

Objectives: The objective was to estimate the impact of the meniscus on cartilage and subchondral bone in knee osteoarthritis (OA).
Methods: In a sample of 46 knee specimens (26 females), 13 (7 females) were classified as OA according to the Kellgren-Lawrence classification. Outerbridge and meniscal grading were performed. Using micro-computed tomography images, we analyzed the cartilage thickness, subchondral plate thickness and micro-architecture of trabecular subchondral bone at different depths and in two different locations of the medial tibial plateau: one peripheral (PER) covered by the meniscus and one central (CENT) uncovered by the meniscus.
Results: Uncoverage by the meniscus was associated with bone sclerosis, defined as higher bone volume to total volume (BV/TV), higher trabecular number, thicker trabeculae with lower spacing, and anisotropy and a more plate-like architecture. The protective effect of meniscal coverage was observed in the uppermost 5 to 6 mm of the subchondral bone. As compared with normal knees, knees with OA showed significantly higher bone sclerosis ($P < 0.05$–0.001) at the PER location, but only BV/TV ($P = 0.03$) and trabecular number ($P = 0.02$) differed between OA and non-OA knees at the CENT location uncovered by meniscus.
Conclusions: OA results showed a partial dedifferentiation of the subchondral bone micro-architecture between PER and CENT locations probably due to menisci that still retain some of their protective effects on the subchondral bone.

1. Introduction

Osteoarthritis (OA) is a multifactorial disease of the whole joint. Various genetic and environmental risk factors and pathophysiologic processes contribute to its gradual progression: degradation of articular cartilage, osteophyte formation, subchondral sclerosis, meniscal degeneration, bone marrow lesions, synovial proliferation and low-grade inflammation (Chen et al., 2017a). Knee OA presents the greatest morbidity (Felson, 2006). In the knee, most commonly the medial compartment is affected (Lawrence et al., 2008).

Cartilage, menisci and subchondral bone are a functional unit. The relationship between bone and cartilage in OA has been widely discussed (Biswal et al., 2002). Although the destruction of articular cartilage seems to be the dominant feature of OA, some researchers suspect that subchondral bone changes may exacerbate cartilage degeneration (Goldring and Goldring, 2010). Sclerosis of subchondral bone is considered one of the primary radiologic features of OA (Altman and Gold, 2007). Menisci play an important role in load-bearing transmission, shock absorption, joint congruity and stability (Fox et al., 2015). Meniscal injury is associated with hyaline cartilage alteration leading to knee OA (Fox et al., 2015). Partial and total meniscectomy is associated with articular degradation and OA progression (Felson, 2013).

Changes in subchondral bone micro-architecture caused by OA have been investigated by 2D histology (Matsui et al., 1997; Bobinac et al., 2003; Finnilä et al., 2017; Chen et al., 2017b) or 3D micro-computed tomography (CT) (Finnilä et al., 2017; Chen et al., 2017b; Patel et al., 2003; Roberts et al., 2017) of tibia plateaus collected during total knee arthroplasty. Two of these studies also included control cadaveric samples (Bobinac et al., 2003; Chen et al., 2017b). Targeted outcomes were location-specific differences in subchondral bone architecture of the tibial plateau (Matsui et al., 1997; Bobinac et al., 2003; Roberts et al., 2017) and variation in the subchondral and trabecular architecture of the epiphysis with increasing distance from the chondro-osseous junction (Matsui et al., 1997; Bobinac et al., 2003). However,

* Corresponding author at: B3OA, 10, avenue de Verdun, 75010 Paris, France.
E-mail address: christine.chappard@inserm.fr (C. Chappard).

https://doi.org/10.1016/j.bonr.2020.100271
Received 25 September 2019; Received in revised form 18 March 2020; Accepted 10 April 2020
Available online 16 May 2020

none of these studies specifically investigated the impact of the meniscus on subchondral architecture.

Bone volume (BV) and trabecular thickness (Tb.Th) were found highest in the superficial layer and decrease with increasing distance from the chondro-osseous junction (Matsui et al., 1997; Bobinac et al., 2003). These findings were confirmed by a micro-CT study of normal and osteoarthritic human knee specimens (age range 59–74 years), which showed a depth dependence of subchondral bone microstructure in the first 6 mm below the subchondral bone plate and differences in microstructure between medial and lateral compartments (Patel et al., 2003). The depth dependence of BV to total volume (BV/TV), Tb. Th, trabecular number (Tb.N) and structure model index (SMI) was also established in our own micro-CT study of the medial compartment of human tibia specimens without OA (mean age 82 ± 10 years) (Touraine et al., 2017). More importantly, our study demonstrated a significant protective effect of the meniscus on cartilage and subchondral bone structure. Cartilage and subchondral bone plate were thicker in the center of the tibial plateau, an area not covered by the meniscus, than in posterior and peripheral locations covered by the meniscus.

However, none of these studies included a 3D combined evaluation of cartilage thickness, subchondral bone plate and trabecular subchondral bone micro-architecture or a location-specific analysis with respect to meniscal coverage. Also, none of the studies included a separate analysis of males and females with age matching between OA and controls, although the dependence of bone micro-structure on age is sex-specific (Lochmüller et al., 2008).

The objective of this study was to estimate the impact of the meniscus on cartilage and subchondral bone in subjects with knee OA compared to controls. We hypothesized that in humans, cartilage thickness and subchondral bone microstructure of the proximal tibia depend on coverage by the meniscus and that the protective effect of the meniscus is reduced or even absent in knees with than without OA.

2. Material and methods

2.1. Specimens

We obtained 46 human unpaired left cadaveric knees (26 females, mean age 86.1 ± 7.7 years; 20 males, mean age 80.0 ± 11.3 years) from the Paris Descartes Anatomy Institute, France. All donors were Caucasian. The study was approved by the Ethics Committee of the Paris Descartes University. These human tissue specimens were collected according to pertinent protocols established by the INSERM Human Ethics Committee. The subjects willed their body to science and were anonymous, so no data were available regarding the cause of death, previous illnesses, or medical treatment.

After soft tissue removal, knee specimens were obtained after cutting the distal third of femoral diaphysis and proximal third tibial diaphysis and were stored at −20 °C. The Kellgren-Lawrence (KL) grade (Kellgren and Lawrence, 1957) was determined from posterior-anterior radiographs taken of the specimens lying on the table (Axiom Luminos, Siemens, Munich, Germany). In total, 33 knees (19 females) graded as KL 0 or 1 were classified as normal and 13 knees (7 females) graded KL 2 to 4 were classified as OA. The sample of 28 knees used in our previous publication (Touraine et al., 2017) was a subsample of the 33 normal knees.

Knees were dissected, and tibial plateaus were excised perpendicular to the longitudinal axis of the tibia at a depth of 3 cm. A second grading system (Pauli et al., 2011) was used to characterize meniscal degeneration by qualifying the macroscopic appearance of the meniscus before removal. Grade 1: Normal intact menisci, attached at both ends with sharp inner borders, no tibial or femoral surface changes. Grade 2: Fraying at inner borders, tibial or femoral surface fibrillation, no tears. Grade 3: Partial substance tear fraying, tibial or femoral side fibrillations. Grade 4: Full/complete substance tears, loss of tissue (Fig. 1a_1, b_1). After meniscus removal, to improve cartilage visualization, joint surfaces were rinsed with saline, stained with waterproof black India ink (Sanford Rotring, Hamburg, Germany), dried for 10 min, and rinsed again to remove the ink from the normal cartilage surface so that only the cartilage fibrillation areas remained dark (Meachim and Fergie, 1975). All joint surfaces were photographed alongside a ruler. Cartilage degradation was assessed by the modified Outerbridge classification (Uhl et al., 1998): Grade 0: normal cartilage; grade 1: cartilage softening and swelling; grade 2: mild surface fibrillation and/or reduction of cartilage thickness by < 50%; grade 3: severe surface fibrillation and/or loss of cartilage thickness by > 50%; grade 4: complete loss of cartilage with subchondral bone exposure.

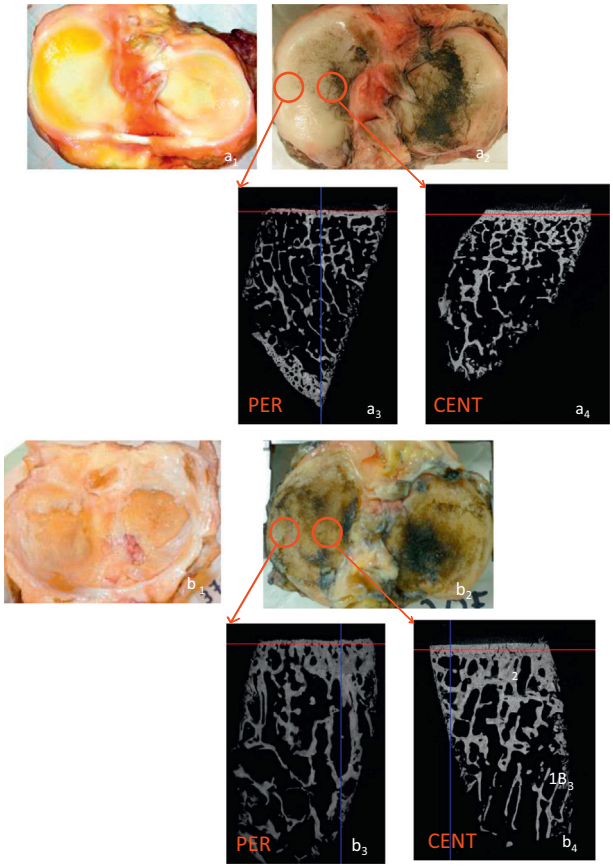

Fig. 1. Tibial plateaus in control specimen (a) and osteoarthritis specimen (b) with (a_1, b_1) and without meniscus (a_2, b_2). Locations of cores used for the analysis of cartilage and subchondral bone characteristics (a_1 and b_1). Post-acquisition rotation of Micro-CT images ensured that each slice was perpendicular to the cartilage surface in areas covered by meniscus: PER (a_3, b_3) and not covered by meniscus: PER (a_4,b_4).

2.2. Sample preparation and micro-CT imaging

Bone cores with an internal diameter of 7 mm trephine were harvested in the medial tibial plateau by use of a circular diamond saw (BROT, Argenteuil, France). The bone cores were harvested in two different areas of the medial tibial plateau (Fig. 1a_2, b_2). A peripheral core (PER) fully covered by the meniscus was located midway between the anterior and posterior edges of the tibial plateau, and a second core was harvested from the center of the tibial plateau (CENT), not covered by the meniscus.

Two micro-CT scans (Skyscan 1172, Bruker Kontich, Belgium) were obtained from each core to optimize cartilage or bone contrast. For the cartilage scan, each core was placed in a plastic tube and put in a bath of mineral oil (Sigma-Aldrich Chemical Co., St Louis, MO) and images

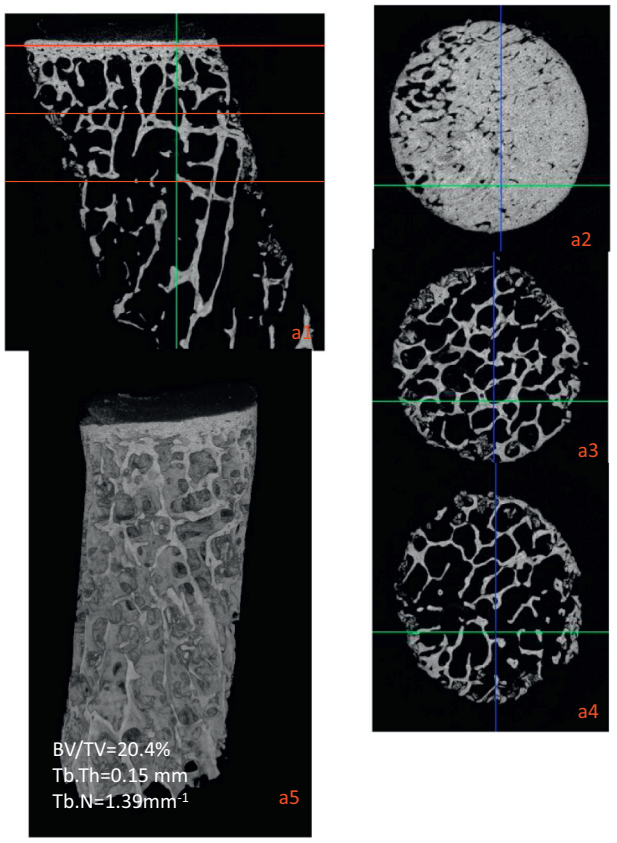

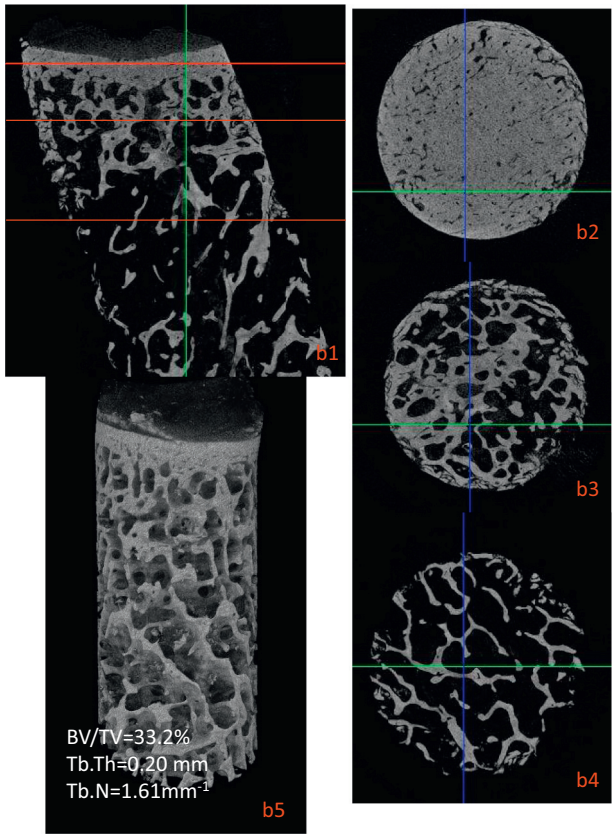

Fig. 2. Examples of subchondral plates and trabecular bone at the CENT location (a) in normal and (b) in osteoarthritic sample. a1 and b1: coronal views with positioning of the slices, a2,b2: transversal views of subchondral plate, a3,b3: trabecular bone in the upper 5 mm, a4,b4:and trabecular bone beyond. a5 and b5: 3D volumes.

Fig. 2. (*continued*)

were acquired at 37 kV and 100 μA, rotation step: 1.2°, 10-frame averaging with acquisition time 16 min. Further details are described elsewhere (Delecourt et al., 2016). For the bone scan, the bone cores were defatted before acquisition with supercritical CO_2, which in a microporous solid diffuses better than solvent and leads to total dilapidation of small bone samples (Fages et al., 1998), Bone images were acquired at 80 kV and 100 μA, with a 0.5-mm-thick aluminum filter, 0.5° per rotation, and 30-frame averaging. Total acquisition time was 1 h20. 3D datasets were reconstructed by using the manufacturer's customized Feldkamp reconstruction algorithm (NReCon, Skyscan, Bruker, Kontich, Belgium). 3D datasets were reconstructed with an isotropic voxel size of 10.2 μm (Fig. 2).

2.3. Cartilage and subchondral bone analysis

As described previously (Delecourt et al., 2016), data were processed by using CtAn (Skyscan, Bruker, Kontich, Belgium). Briefly, for determining cartilage thickness (Cart_Th, mm) the surfaces were contoured manually. Thickness was then determined by using the method of largest spheres that could be positioned inside (Hildebrand and Ruegsegger, 1997).

The tibial plateau is usually not perpendicular to the tibial axis, and this angle depends on the location where the core is extracted. Therefore, the micro-CT datasets were rotated (Dataviewer, Bruker, Kontich, Belgium) to ensure that in a slice-by-slice analysis, each slice was parallel to the cartilage surface. (Fig. 1a_3,a_4; b_3,b_4). For measuring cortical subchondral plate thickness (SBP_Th, mm), the same technique as for the cartilage analysis was used: manual segmentation combined with the sphere method.

Subchondral bone structure was segmented by using a threshold of 60 (0–255) for all datasets. Trabecular architecture was determined in each core by using 3 circular volumes of interest (VOIs) (ø = 6 mm), one extending from 1 to 5 mm beneath the plate, one from 6 to 10 mm and a third from 11 to 15 mm. The following subchondral bone structure parameters were determined: BV/TV (%), Tb.N (mm-1), Tb.Th (mm), trabecular spacing (Tb.Sp, mm), and SMI, which quantifies plates versus rods: values of 0 for a perfect plate structure and 3 for a perfect rod structure. Finally, the degree of anisotropy (DA) defines the orientation of the trabecular structure: DA is 1 for isotropic structures and is > 1 for anisotropic structures. Further details have been described elsewhere (Touraine et al., 2017).

2.4. Statistical analysis

Unpaired *t*-tests (Wilcoxon test in case of non-normality) were used to determine group differences between OA and normal knees for all parameters listed above. Paired t-tests were used to compare results between the PER and CENT locations. ANOVA (Kruskall Wallis in case of non-normality) was used to compare OA and normal knee samples obtained at the 3 different depths beneath the subchondral plate, followed by multiple-comparison post-hoc Bonferroni correction. A Mann Whitney test was used to compare the Outerbridge and meniscal grades in normal and OA knees. All statistical analyses were performed with NCSS software (NCSS, Kaysville, UT).

The difference between PER and CENT locations was computed as a percentage:

$$\langle \Delta \ bone\ parameter \rangle = \frac{100}{n} \sum_{i=1}^{i=n} \frac{|bone\ parameter\ PER - bone\ parameter\ CENT|}{bone\ parameter\ PER} \quad (1)$$

Table 1
Mean ± SD of cartilage thickness, subchondral bone plate thickness and trabecular bone micro-architecture measured at 1to 5 mm beneath the subchondral plate, comparison between OA subjects and controls and comparison between the CENT and PER positions.

1–5 mm	Central position not covered (CENT)			Peripheral position under meniscus (PER)			Comparisons CENT/PER			
	OA	Normals	*P* value OA/ normals	OA	Normals	P value OA/ normals	P value OA	P value Normals	% diff OA	%diff Normals
Males	(n = 6)	(*n* = 14)		(n = 6)	(n = 14)					
Cart_Th (mm)	1.34 ± 0.38	2.20 ± 0.5	0.0007	1.55 ± 0.40	1.84 ± 0.35	ns	ns	0.02	35.0	20.6
SBP_Th (mm)	0.54 ± 0.12	0.61 ± 0.20	ns	0.45 ± 0.15	0.42 ± 0.20	ns	ns	0.008	47.4	74.1
BV/TV(%)	42.7 ± 4.8	34.9. ± 8.5	0.03	34.8 ± 9.4	23.2 ± 5.7	0.001	0.05	0.03	33.2	54.5
Tb.Th(mm)	0.23 ± 0.02	0.21 ± 0.04	ns	0.21 ± 0.02	0.16 ± 0.03	0.001	0.03	0.001	13.4	29.6
Tb.N(1/mm)	1.83 ± 0.26	1.63 ± 0.15	0.02	1.65 ± 0.32	1.39 ± 0.16	0.01	ns	0.0002	18.8	19.2
Tb.Sp(mm)	0.44 ± 0.09	0.50 ± 0.05	ns	0.50 ± 0.06	0.55 ± 0.06	0.05	ns	0.02	14.5	9.4
SMI	−0.02 ± 1.0	0.10 ± 0.46	ns	0.02 ± 1.31	0.85 ± 0.34	0.02	ns	0.0001	59.1	102.5
DA	1.43 ± 0.08	1.38 ± 0.21	ns	1.59 ± 0.28	1.89 ± 0.31	ns	ns	$< 10^{-4}$	12.3	26.0
Females	(n = 7)	(*n* = 19)		(n = 7)	(n = 19)					
Cart_Th (mm)	1.94 ± 0.97	2.14 ± 0.38	ns	1.14 ± 0.54	1.68 ± 0.20	0.02	0.04	0.0002	40.7	78.8
SBP_Th (mm)	0.65 ± 0.12	0.66 ± 0.14	ns	0.56 ± 0.20	0.39 ± 0.15	ns	ns	0.0004	189	35.1
BV/TV(%)	27.6 ± 3.5	22.9 ± 6.9	0.05	23.3 ± 4.1	16.8 ± 6.5	0.01	0.003	0.001	20.3	61.4
Tb.Th(mm)	0.18 ± 0.02	0.16 ± 0.02	ns	0.16 ± 0.02	0.14 ± 0.03	0.01	0.005	0.0003	10.1	27.3
Tb.N(1/mm)	1.53 ± 0.09	1.36 ± 0.27	0.01	1.41 ± 0.16	1.18 ± 0.25	0.02	0.05	0.01	10.7	25.9
Tb.Sp(mm)	0.53 ± 0.04	0.57 ± 0.1	ns	0.53 ± 0.06	0.60 ± 0.10	ns	ns	ns	4.5	13.2
SMI	0.56 ± 0.40	0.94 ± 0.40	0.02	0.96 ± 0.37	1.22 ± 0.42	ns	0.001	0.007	52.5	40.2
DA	1.49 ± 0.21	1.53 ± 0.26	ns	1.93 ± 0.42	1.93 ± 0.45	ns	ns	0.001	25.7	24.4

Unpaired *t*-tests (Wilcoxon test in case of non-normality) were used to determine group differences between OA and normal knees. Paired *t*-tests were used to compare results between the PER and CENT locations.
Differences in percent of CENT relative to PER.

3. Results

The mean age was 80.6 ± 7.0 for males with normal knees (normal males) versus 79.6 ± 12.9 years for males with OA knees (OA males), and 85.7 ± 6.0 for normal females versus 86.2 ± 8.3 years for OA females; mean ages were not statistically different for both sexes. Outerbridge grades were distributed as follows: for normal males, Gr1 $n = 5$, Gr2 $n = 9$; for OA males, Gr2 $n = 2$, Gr3 n = 2, Gr4 n = 2; for normal females, Gr 1 $n = 11$, Gr2 $n = 6$, Gr3 n = 2; for OA females, Gr3 n = 2 and Gr4 $n = 5$. Outerbridge grades (grades 3 and 4 in 85% of cases) were significantly higher for OA than normal knees (grades 1 and 2 in 94% of cases) ($p < 0.001$). Meniscal grades were distributed as follows: for normal males, Gr1 n = 9, Gr2 $n = 4$, Gr3 n = 1; for OA males, Gr2 n = 1, Gr3 n = 2, Gr4 $n = 3$; for normal females, Gr 1 $n = 12$, Gr2 $n = 7$; for OA females, Gr2 n = 1, Gr3 n = 1 and Gr4 n = 5. Meniscal grades (grades 3 or 4 in 85% of cases) were significantly higher for OA than normal knees (grade 1 or 2 in 97% of cases) ($p < 0.001$).

Results for Cart_Th, SBP_Th and subchondral bone structure of the uppermost 5 mm are detailed in Table 1.

In general, in OA knees BV/TV, Tb.N, and Tb.Th were numerically higher and Cart_Th, Tb.Sp and SMI numerically lower than in normal knees, independent of location and sex, however differences were consistently significant for BV/TV and Tb.N only. Differences in SBP_Th, DA and Tb.Sp (with one exception) between OA and normal knees were not significant independent of location and sex.

The SMI results indicate a more plate-like trabecular bone structure in OA than normal knees, but again, not all differences were significant.

In normal knees of both sexes, Cart_Th and SBP_Th were higher and all five subchondral bone architecture parameters differed significantly between the two locations, with higher trabecular bone volume, thickness, and number and lower spacing, SMI and DA at the CENT than PER location. Mean differences in subchondral bone architecture parameters between PER and CENT locations showed similar trends in normal and OA knees. However, differences were lower and not consistently significant in OA knees (Table 1). In absolute terms the % difference between central and peripheral locations was about halved for BV/TV and Tb.Th in OA versus normal knees for both sexes (BV/TV: 54.5% versus 33.2% in males; 61.4% versus 20.3% in females). Tb.Th: 29.6% versus 13.4% in males; 27.3% versus 10.1% in females. Results for the other parameters were more disparate.

Because female donors were 5 to 6 years older than males, on average, and loading conditions in males and females may differ, we did not compare results between males and females. However, differences in trabecular architecture between OA and normal knees and between PER and CENT locations showed the same trends in females and males.

The depth dependence of the subchondral bone architecture parameters is shown in Fig. 3 for males and Fig. 4 for females. All parameters significantly differed ($P = 0.04–10^{-4}$) between the subchondral bone close to the joint (1–5 mm) and the other two depth ranges (6–10 and 11–15 mm), with no significant differences between the 6–10 and 11–15 mm depths. An illustration of normal and OA specimens is in Fig. 2.

Results of trabecular bone structure at the two deeper locations are shown in Table 2. Differences between OA and normal knees were no longer significant at the CENT location (except Tb.Sp at 6–10 mm for males). However, at the PER location, differences remained significant for BV/TV and Tb.Th for both males and females at the 6–10 mm depth and only for males at the 11–15 mm depth. Differences between CENT and PER locations persisted for some parameters in normal but not OA knees, except for female OA knees at 11–15 mm depth.

4. Discussion

In this study, we have extended our earlier investigation on the protective effect of the meniscus on subchondral bone and cartilage in elderly subjects without OA (Touraine et al., 2017) to subjects with OA. In OA subjects a significantly higher deterioration of cartilage and meniscus was observed, yet even a deteriorated meniscus retained some protective effect against osteoarthritis-induced subchondral bone changes. Earlier studies including our own have reported a protective effect of the meniscus on subchondral bone (Touraine et al., 2017) in subjects without OA and in a recent in vivo study in subjects with OA as well (Sannmann et al., 2020) as a protective effect of the meniscus on the hyaline cartilage in pigs (Iijima et al., 2014).

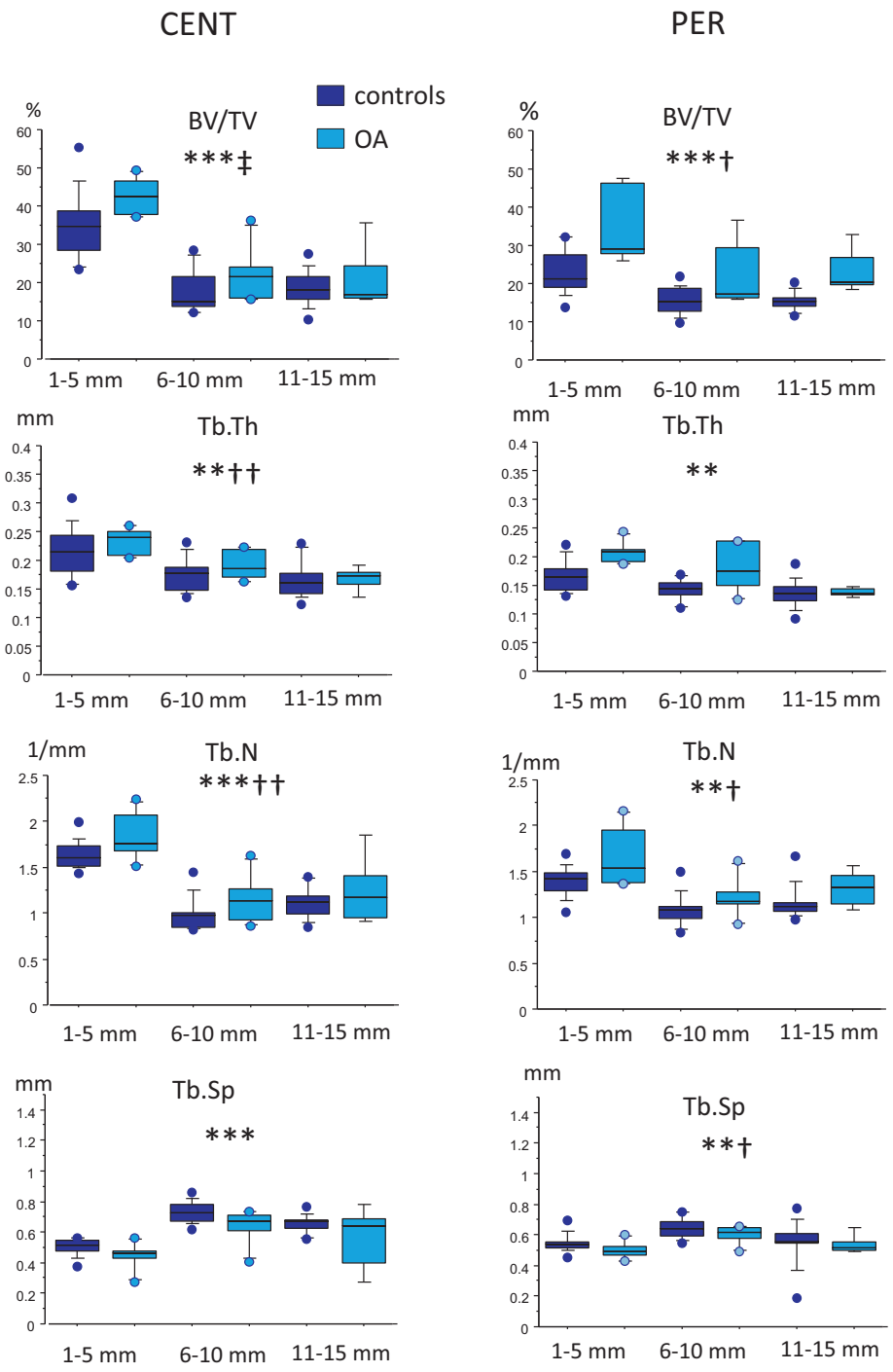

Fig. 3. Individual values of morphological and topological trabecular bone parameters in males according to location in the tibial plateau: PER (covered by meniscus) and CENT (not covered by meniscus) and by depth: 1–5, 6–10 and 11–15 mm. ANOVA or a Kruskall Wallis *in italics* (in case of non-normality).

In the current study, advanced grades of cartilage and meniscal degeneration (grades 3 and 4) were associated with subchondral bone sclerosis, defined as higher BV/TV, higher Tb.N, thicker trabeculae with lower spacing and a more plate-like architecture. These new results agree with recent data from specimens obtained after total knee replacement showing higher BV/TV, Tb.Th, and Tb.N and lower SMI in specimens with high versus low OARSI grades (Finnilä et al., 2017). Another study included a biomechanical perspective by showing that subchondral bone sclerosis was associated with subchondral bone stiffening in the presence of reduced matrix mechanical properties (Day et al., 2004), however, the effect of the meniscus was not investigated. In contrast, in our study biomechanical parameters were not included.

We performed a detailed mapping of the subchondral bone architecture based on 3D micro-CT imaging. Not surprisingly the differences in subchondral bone structure between PER and CENT locations in control knees reported in our earlier study (Touraine et al., 2017) were confirmed as the investigated specimen largely overlapped. These differences indicated a bone adaptation to an increase in contact stress in the CENT location (Ahmed and Burke, 1983). As compared with normal knees, OA knees showed significantly higher bone sclerosis at the PER location, but the effect of OA was pronounced at the CENT location uncovered by meniscus.

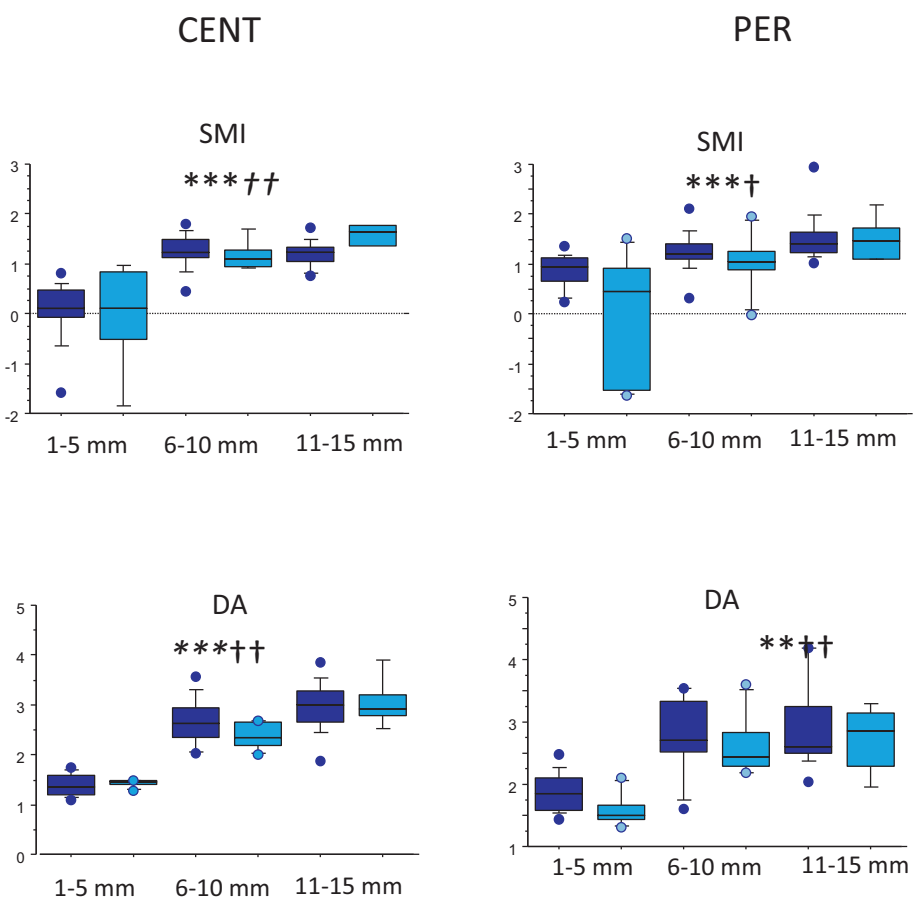

Fig. 3. (*continued*)

For males and females, the differences between PER and CENT locations were two times higher in normal than in OA for BV/TV, Tb.Th and only in females for Tb.N. Thus, despite higher damage of the meniscus, some protective effect on subchondral bone was still observed in OA knees, in particular when comparing BV/TV and Tb.Th at the PER and CENT locations, indicating a lower degree of sclerosis at the PER location also in OA knees. Of course, OA is the dominant cause of bone sclerosis and the meniscus does not protect from potential OA maladaptation but the protection of the meniscus against increased contact stresses observed in normal knees is at least partly retained in OA.

This protective effect of the meniscus on subchondral bone is predominant at the uppermost 5–6 mm (Figs. 3 and 4), with a small impact of the deeper areas of the trabecular bone. In the present study, we have also observed mean differences between OA and controls in this region. This finding suggests that the uppermost 5–6 mm subchondral bone plays a major role in load absorption in OA. This tendency was already observed in two histological studies and one micro-CT study (Matsui et al., 1997; Bobinac et al., 2003; Patel et al., 2003). Moreover, the ultimate strength of the proximal tibia abruptly decreased 5 mm below the surface (Harada et al., 1988). A layer of 5 mm can be imaged in vivo by using standard whole-body CT scanners (Lowitz et al., 2017).

In control knees, Cart_Th was about 20% thicker at the CENT than the PER location. As expected, Cart_Th is reduced in OA, but differences between OA and control knees were not always significant. Interestingly, we did not observe a significant effect of OA on SBP_Th, contrary to the classical description of thinning of SBP with increasing porosity, which is typically observed as an early adaptation in animal models of post-traumatic OA (Li et al., 2013).

In normal specimens, DA was higher at the PER than CENT site for both males and females in the uppermost 5 mm. The same trend was observed for OA specimens, but differences were not significant probably because of the small sample size. Architectural anisotropy characterizes the degree of directional organization of a material and is of particular relevance to mechanics–architecture relations (Odgaard, 1997). Higher DA values indicate that the orientation more closely parallels the main direction of the compression forces, with few transverse trabeculae parallel to the cartilage surface. This orientation may decrease the ability of the subchondral bone to transmit shear stresses at the PER versus CENT site and may indicate a decrease in shear stress from the surface to the depth, consistent with a more uniform trabecular network composed mainly of vertical trabeculae. Interestingly these results agree quite well with the FE-based bone anisotropic theory proposed by Doblaré and García (Doblaré and Garcıa, 2001) for the proximal femur. In the OA group, the differences between the PER and CENT sites persisted also indicating the absence of more horizontal trabeculae. Apparently, the position under the meniscus and not the presence of OA is the main determinant of anisotropy.

The experimental conditions to study the bone microarchitecture were optimized. The defatting of bone ensured very high image quality, histograms were clearly biphasic, and we could use the same segmentation threshold for all datasets. The bone micro-architectural parameters obtained by using similar conditions with desktop micro-CT were close to those obtained by synchrotron radiation micro-CT (Chappard et al., 2006). Also, according to earlier recommendations, the voxel size of 10 μm was adequate for an accurate analysis of trabecular bone architecture (Peyrin et al., 1998).

The main limitation of our study was the small sample size, especially the number of OA knees, which may have affected significance, however, despite this limitation the observation of a protective effect of meniscus remains valid. Also, female donors were older than male donors, which complicated a comparison between the sexes. We performed a sex-specific analysis in our study because pooling data for the

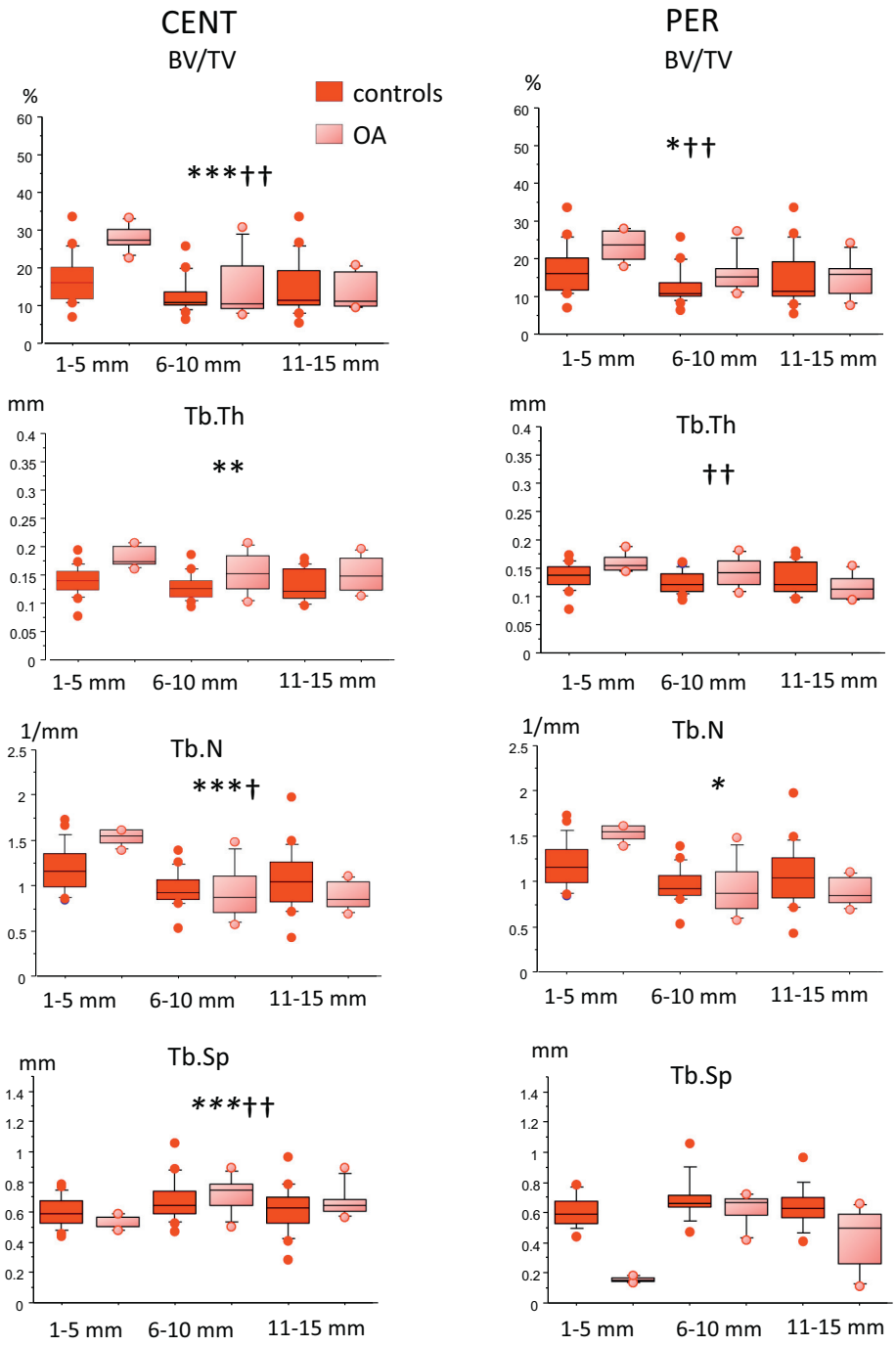

Fig. 4. Individual values of morphological and topological trabecular bone parameters in females according to location in the tibial plateau: PER (covered by meniscus) and CENT (not covered by meniscus) and by depth: 1–5, 6–10 and 11–15 mm. ANOVA test or Kruskall Wallis *in italics* (in case of non-normality).

sexes would lead to misinterpretation. For example, in the VOIs located in PER area within 5 mm below the chondro-osseous junction, the mean BV/TV and Tb.Th were 23% and 0.16 mm, respectively, in both OA females and normal males. In most histological studies, males and females were not analyzed separately (Matsui et al., 1997; Bobinac et al., 2003; Finnilä et al., 2017; Chen et al., 2017b).

Bone micro-structure is sex- but also age-specific (Lochmüller et al., 2008). In the present study, we did not find any correlation with age. One may speculate that large variations in mechanical loading dominate the age dependency, but we did not determine mechanical loading. Also, the age range was relatively narrow. Indeed, the mean age of adults was about 86 years for females and 80 years for males. Therefore, our results cannot be completely extrapolated to a 50-year-old population.

In our study ages were similar for both male and female OA and normal specimens. In most studies, the age and sex ratio were not taken into account. For example, in the Bobinac et al. study, the average age of OA patients was 62 years, with a sex ratio of 7 females to 3 males and the average age of control cadavers was 47 years, with a sex ratio of 3 females to 7 males.

Another limitation of the study was lack of information on prior medications and injury status of cadavers, which could not be obtained according to legal regulations and ethical issues. Moreover, we had no information on knee alignment, although the distribution of the

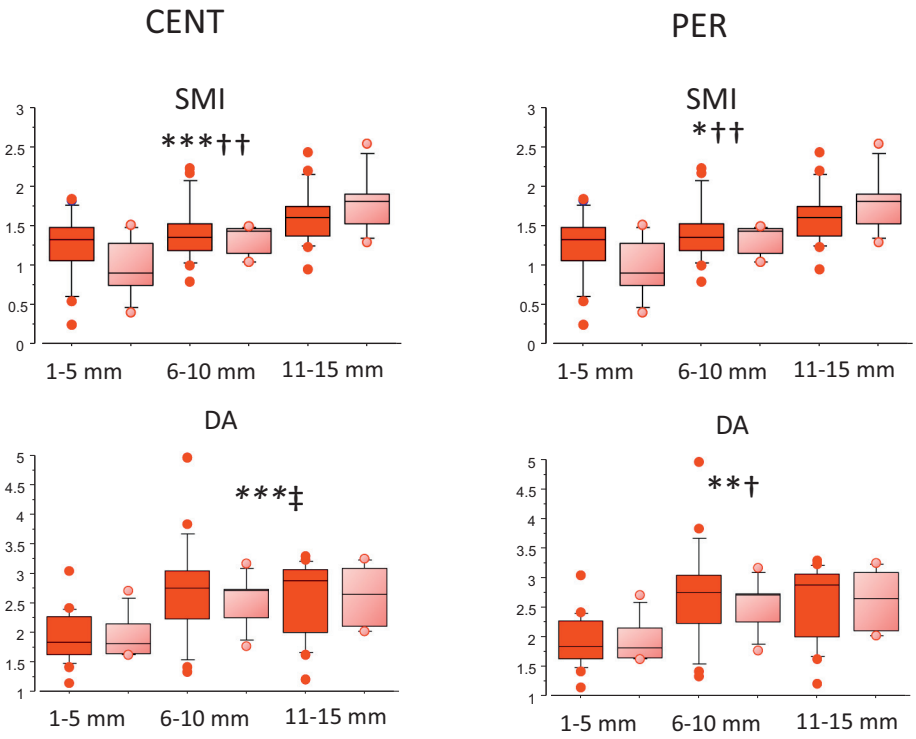

Fig. 4. (*continued*)

Table 2
mean ± SD of subchondral trabecular bone micro-architecture measured at 6 to 10 mm and 11 to 15 mm beneath the subchondral plate, comparison between OA subjects and controls and comparison between the CENT and PER positions.

	Central position not covered (CENT)			Peripheral position under meniscus (PER)			Comparisons CENT/PER	
	OA	Controls	P value OA/controls	OA	Controls	P value OA/controls	P value OA	P value controls
Males								
6–10 mm	(n = 6)	(n = 14)		(n = 6)	(n = 14)			
BV/TV(%)	22.4 ± 7.6	17.5 ± 5.4	ns	22.2 ± 8.2	15.6 ± 3.5	ns	ns	ns
Tb.Th(mm)	0.19 ± 0.02	0.17 ± 0.03	ns	0.18 ± 0.04	0.14 ± 0.02	0.04	ns	0.003
Tb.N(1/mm)	1.16 ± 0.27	0.98 ± 0.17	ns	1.22 ± 0.23	1.08 ± 0.16	ns	ns	0.03
Tb.Sp(mm)	0.63 ± 0.12	0.73 ± 0.07	0.02	0.60 ± 0.06	0.64 ± 0.06	ns	ns	ns
SMI	1.15 ± 0.27	1.25 ± 0.33	ns	1.03 ± 0.64	1.25 ± 0.40	ns	ns	ns
	2.37 ± 0.27	2.67 ± 0.45		2.63 ± 0.52	2.74 ± 0.64	ns		
11–15 mm	(n = 5)	(n = 14)		(n = 6)	(n = 14)			
BV/TV(%)	20.9 ± 8.4	18.4 ± 4.7	ns	22.1 ± 6.0	15.7 ± 2.4	0.02	ns	0.03
Tb.Th(mm)	0.17 ± 0.02	0.16 ± 0.03	ns	0.17 ± 0.03	0.14 ± 0.02	0.01	ns	0.01
Tb.N(1/mm)	1.23 ± 0.37	1.15 ± 0.17	ns	1.27 ± 0.20	1.15 ± 0.14	ns	ns	ns
Tb.Sp(mm)	0.59 ± 0.20	0.66 ± 0.06	ns	0.55 ± 0.08	0.55 ± 0.13	ns	ns	0.001
SMI	1.45 ± 0.35	1.20 ± 0.26	ns	1.41 ± 0.44	1.51 ± 0.49	ns	ns	ns
DA	3.04 ± 0.51	2.97 ± 0.49	ns	2.85 ± 0.58	2.91 ± 0.66	ns	ns	ns
Females								
6–10 mm	(n = 7)	(n = 19)		(n = 7)	(n = 19)			
BV/TV(%)	15.1 ± 8.4	12.6 ± 5.2	ns	15.9 ± 5.4	12.5 ± 4.6	0.02	ns	ns
Tb.Th(mm)	0.15 ± 0.03	0.14 ± 0.02	ns	0.14 ± 0.02	0.13 ± 0.02	ns	ns	0.005
Tb.N(1/mm)	0.93 ± 0.31	0.85 ± 0.23	ns	1.08 ± 0.20	0.96 ± 0.19	ns	ns	0.003
Tb.Sp(mm)	0.72 ± 0.12	0.79 ± 0.15	ns	0.64 ± 0.10	0.63 ± 0.10	ns	ns	0.008
SMI	1.38 ± 0.41	1.41 ± 0.47	ns	1.41 ± 0.37	1.33 ± 0.4	ns	ns	ns
DA	2.30 ± 0.46	2.61 ± 0.55	ns	2.51 ± 0.45	2.70 ± 0.85	ns	ns	nd
11–15 mm	(n = 7)	(n = 19)		(n = 7)	(n = 17)			
BV/TV(%)	13.9 ± 5.0	13.3 ± 5.4	ns	14.9 ± 5.4	14.5 ± 7.5	ns	ns	ns
Tb.Th(mm)	0.15 ± 0.03	0.14 ± 0.02	ns	0.12 ± 0.02	0.13 ± 0.03	ns	0.01	ns
Tb.N(1/mm)	0.90 ± 0.16	0.95 ± 0.29	ns	1.24 ± 0.44	1.06 ± 0.35	ns	0.04	ns
Tb.Sp(mm)	0.67 ± 0.10	0.68 ± 0.14	ns	0.46 ± 0.20	0.62 ± 0.15	ns	0.01	0.02
SMI	1.68 ± 0.26	1.52 ± 0.40	ns	1.78 ± 0.39	1.56 ± 0.37	ns	ns	ns
DA	2.49 ± 0.43	2.94 ± 0.62	ns	2.48 ± 0.47	2.57 ± 0.63	ns	ns	ns

Unpaired *t*-tests (Wilcoxon test in case of non-normality) were used to determine group differences between OA and normal knees. Paired *t*-tests were used to compare results between the PER and CENT locations.

subchondral bone superficial layers across the medial tibial plateau depends on the varus degree (Roberts et al., 2017). We can expect a maximum varus malaligment of 20°, as reported in a large Caucasian cohort (Brouwer et al., 2007). In most studies, OA specimens were retrieved from patients who underwent total knee arthroplasty and had endstage OA (Matsui et al., 1997; Bobinac et al., 2003; Roberts et al., 2017). In our study, we had only a few endstage grade 4 cartilage defects corresponding to late-stage OA: $n = 2$ males and $n = 4$ females. Nevertheless, we found significant differences between normal and OA knees. The lack of significant differences within the OA group can be due in part to discrepancies between the KL classification and histopathological grades. For the diagnosis of OA the KL classification was used, which provided information on bone sclerosis, osteophytes and bony deformation. As the KL score is less indicative for cartilage damage, the Outerbridge classification was applied for a more pertinent evaluation of cartilage state. Indeed, in two males of the OA group, there was a discrepancy between KL classification (KL = 3) and Outerbridge classification Gr2; the joint space narrowing in these cases was due to damaged menisci (Gr4). Indeed, meniscal impairment is known to reduce the joint space (Fox et al., 2015). In two normal female knees with KL = 0 and KL = 1, we found local cartilage defects, so the Outerbridge classification was 3.

5. Conclusion

The effect of knee OA on subchondral bone microarchitecture is location specific requiring a 3D imaging procedure. In normal knees the meniscus has a protective effect on subchondral bone. In OA knees, differences in subchondral bone structure decreased but persisted between locations under and not under the meniscus, which indicates a tendency to dedifferentiation. Consequently, even in OA, degenerated meniscus still retains some protective effects on subchondral bone, that confirms the need to limit as much as possible the resection of the medial meniscus in OA.

Transparency document

The Transparency document associated with this article can be found, in online version.

Acknowledgments

None.

Author contributions

Conception and design (CC,JDL,KE), analysis and interpretation of the data (CC,JDL,KE), drafting of the article (CC,KE), critical revision of the article for important intellectual content (all authors), final approval of the article (all authors), provision of study material or patients (CC, JDL), obtained funding (JDL,CC), collection and assembly of data (CC,GM).

Role of funding source

ANR MODOS N° ANR-09-TECS-018. The funding bodies had no role in the study design, collection, analysis and interpretation of data, nor in the writing of the manuscript, or in the decision to submit the manuscript for publication.

Declaration of competing interest

None of the authors has any competing interests to declare.

References

Ahmed, A.M., Burke, D.L., 1983. In-vitro measurement of static pressure distribution in synovial joints—part I: Tibial surface of the knee. J. Biomech. Eng. 105, 216–225 (PMID 6688842).

Altman, R.D., Gold, G.E., 2007. Atlas of individual radiographic features in osteoarthritis, revised. Osteoarthr. Cartil. 15 (Suppl A), A1–56.

Biswal, S., Hastie, T., Andriacchi, T., Bergman, G.A., Dillingham, M.F., Lang, P., 2002. Risk factors for progressive cartilage loss in the knee: a longitudinal magnetic resonance imaging study in forty-three patients. Arthritis Rheum. 46, 2884–2892.

Bobinac, D., Spanjol, J., Zoricic, S., Maric, I., 2003. Changes in articular cartilage and subchondral bone histomorphometry in osteoarthritic knee joints in humans. Bone 32, 284–290.

Brouwer, G.M., van Tol, A.W., Bergink, A.P., Belo, J.N., Bernsen, R.M., Reijman, M., Pols, H.A., 2007. Association between valgus and varus alignment and the development and progression of radiographic osteoarthritis of the knee. Arthritis Rheum. 56, 1204–1211.

Chappard, C., Basillais, A., Benhamou, L., Bonassie, A., Brunet-Imbault, B., Bonnet, N., Peyrin, F., 2006. Comparison of synchrotron radiation and conventional X-ray microcomputed tomography for assessing trabecular bone microarchitecture of human femoral heads. Med. Phys. 33, 3568–3577.

Chen, D., Shen, J., Zhao, W., Wang, T., Han, L., Hamilton, J.L., Im, H.J., 2017a. Osteoarthritis: toward a comprehensive understanding of pathological mechanism. Bone Res 17, 16044. Review. https://doi.org/10.1038/boneres.2016.44.

Chen, Y., Huang, Y.C., Yan, C.H., Chiu, K.Y., Wei, Q., Zhao, J., Guo, X.E., Leung, F., Lu, W.W., 2017b. Abnormal subchondral bone remodeling and its association with articular cartilage degradation in knees of type 2 diabetes patients. Bone Res. 5, 17034. https://doi.org/10.1038/boneres.2017.34. (eCollection 2017).

Day, J.S., Van Der Linden, J.C., Bank, R.A., Ding, M., Hvid, I., Sumner, D.R., Weinans, H., 2004. Adaptation of subchondral bone in osteoarthritis. Biorheology 41, 359–368 (Review).

Delecourt, C., Relier, M., Touraine, S., Bouhadoun, H., Engelke, K., Laredo, J.D., Chappard, C., 2016. Cartilage microstructure assessed by high resolution microcomputed tomography in non OA knees. Osteoarthr. Cartil. 24, 567–571. https://doi.org/10.1016/j.joca.2015.10.009. (Epub 2015 Oct 24).

Doblaré, M., Garcıa, J.M., 2001. Application of an anisotropic bone-remodelling model based on a damage-repair theory to the analysis of the proximal femur before and after total hip replacement. J. Biomech. 34 (9), 1157–1170.

Fages, J., Jean, E., Frayssinet, P., Mathon, D., Poirier, B., Autefage, A., Larzul, D., 1998. Bone allografts and supercritical processing: effects on osteointegration and viral safety. J. Supercrit. Fluids 13, 351–356.

Felson, D.T., 2006. Clinical practice. Osteoarthritis of the knee. N. Engl. J. Med. 354, 841–848 (Review. Erratum in: N Engl J Med. 2006 Jun 8;354(23):2520).

Felson, D.T., 2013. Osteoarthritis as a disease of mechanics. Osteoarthr. Cartil. 21, 10–15. Review. https://doi.org/10.1016/j.joca.2012.09.012.

Finnilä, M.A.J., Thevenot, J., Aho, O.M., Tiitu, V., Rautiainen, J., Kauppinen, S., Nieminen, M.T., Pritzker, K., Valkealahti, M., Lehenkari, P., Saarakkala, S., 2017. Association between subchondral bone structure and osteoarthritis histopathological grade. J. Orthop. Res. 35, 785–792. https://doi.org/10.1002/jor.23312.

Fox, A., Wanivenhaus, F., Burge, A., Warren, R.F., Rodeo, S.A., 2015. The human meniscus: a review of anatomy, function, injury, and advances in treatment. Clin. Anat. 28, 269–287. https://doi.org/10.1002/ca.22456.

Goldring, M.B., Goldring, S.R., 2010. Articular cartilage and subchondral bone in the pathogenesis of osteoarthritis. Ann. N. Y. Acad. Sci. 1192, 230–237 (Review).

Harada, Y., Wevers, H.W., Cooke, T.D., 1988. Distribution of bone strength in the proximal tibia. J. Arthroplast. 31, 167–175.

Hildebrand, T., Ruegsegger, P., 1997. A new method for the model independent assessment of thickness in three dimensional images. J. Microsc. 185, 67–75.

Iijima H, Aoyama T, Ito A, Tajino J, Nagai M, Zhang X, Yamaguchi S, Akiyama H, Kuroki H. Immature articular cartilage and subchondral bone covered by menisci are potentially susceptive to mechanical load. BMC Musculoskelet. Disord. 26 (2014) 15:101. doi: https://doi.org/10.1186/1471-2474-15-101.

Kellgren, J.H., Lawrence, J.S., 1957. Radiological assessment of osteo-arthrosis. Ann. Rheum. Dis. 164, 94–502.

Lawrence, R.C., Felson, D.T., Helmick, C.G., Arnold, L.M., Choi, H., Deyo, R.A., Gabriel, S., Hirsch, R., Hochberg, M.C., Hunder, G.G., Jordan, J.M., Katz, J.N., Kremers, H.M., Wolfe, F., 2008. National Arthritis Data Workgroup. Estimates of the prevalence of arthritis and other rheumatic conditions in the United States. Part 2. Arthritis Rheum. 58, 26–35. https://doi.org/10.1002/art.23176.

Li, G., Yin, J., Gao, J., Cheng, T.S., Pavlos, N.J., Zhang, C., Zheng, M.H., 2013. Subchondral bone in osteoarthritis: insight into risk factors and microstructural changes. Arthritis Res. Ther. 15, 223. Review. https://doi.org/10.1186/ar4405.

Lochmüller, E.M., Matsuura, M., Bauer, J., Hitzl, W., Link, T.M., Müller, R., Eckstein, F., 2008. Site-specific deterioration of trabecular bone architecture in men and women with advancing age. J. Bone Miner. Res. 23, 1964–1973. https://doi.org/10.1359/jbmr.080709.

Lowitz, T., Museyko, O., Bousson, V., Chappard, C., Laouisset, L., Laredo, J.D., Engelke, K., 2017. Advanced Knee Structure Analysis (AKSA): a comparison of bone mineral density and trabecular texture measurements using computed tomography and high-resolution peripheral quantitative computed tomography of human knee cadavers. Arthritis Res Ther. 19 (1), 1. https://doi.org/10.1186/s13075-016-1210-z. 10.

Matsui, H., Shimizu, M., Tsuji, H., 1997. Cartilage and subchondral bone interaction in osteoarthrosis of human knee joint: a histological and histomorphometric study. Microsc. Res. Tech. 37, 333–342.

Meachim, G., Fergie, I.A., 1975. Morphological patterns of articular cartilage fibrillation.

J. Pathol. 115, 231–248.
Odgaard, A., 1997. Three-dimensional methods for quantification of cancellous bone architecture. Bone 20, 315–328.
Patel, V., Issever, A.S., Burghardt, A., Laib, A., Ries, M., Majumdar, S., 2003. MicroCT evaluation of normal and osteoarthritic bone structure in human knee specimens. J. Orthop. Res. 21, 6–13. https://doi.org/10.1016/S0736-0266(02)00093-1.
Pauli, C., Grogan, S.P., Patil, S., Otsuki, S., Hasegawa, A., Koziol, J., Lotz, M.K., D'Lima, D.D., 2011. Macroscopic and histopathologic analysis of human knee menisci in aging and osteoarthritis. Osteoarthr. Cartil. 19, 1132–1141. https://doi.org/10.1016/j.joca.2011.05.008.
Peyrin, F., Salome, M., Cloetens, P., Laval-Jeantet, A.M., Ritman, E., Rüegsegger, P., 1998. MicroCT examinations of trabecular bone samples at different resolutions: 14, 7 and 2 micron level. Technol. Health Care 6, 391–401.
Roberts, B.C., Thewlis, D., Solomon, L.B., Mercer, G., Reynolds, K.J., Perilli, E., 2017. Systematic mapping of the subchondral bone 3D microarchitecture in the human tibial plateau: variations with joint alignment. J. Orthop. Res. 35, 1927–1941. https://doi.org/10.1002/jor.23474.
Sannmann, F., Laredo, J.D., Chappard, C., Engelke, K., 2020. Impact of meniscal coverage on subchondral bone mineral density of the proximal tibia in female subjects - a cross-sectional in vivo study using QCT. Bone 134, 115292.
Touraine, S., Bouhadoun, H., Engelke, K., Laredo, J.D., Chappard, C., 2017. Influence of meniscus on cartilage and subchondral bone features of knees from older individuals: a cadaver study. PLoS One 12 (8), e0181956. https://doi.org/10.1371/journal.pone.0181956. Aug 10.
Uhl, M., Allmann, K.H., Tauer, U., Laubenberger, J., Adler, C.P., Ihling, C., Langer, M., 1998. Comparison of MR sequences in quantifying in vitro cartilage degeneration in osteoarthritis of the knee. Br. J. Radiol. 71, 291–296.